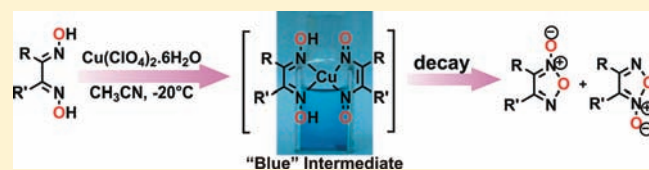


Copper(II)-Mediated Oxidative Transformation of *vic*-Dioxime to Furoxan: Evidence for a Copper(II)-Dinitrosoalkene IntermediateOindrila Das,[†] Sayantan Paria,[†] Ennio Zangrando,[‡] and Tapan Kanti Paine^{†,*}[†]Department of Inorganic Chemistry, Indian Association for the Cultivation of Science, 2A & 2B Raja S. C. Mullick Road, Jadavpur, Kolkata-700032, India[‡]Dipartimento di Scienze Chimiche e Farmaceutiche, University of Trieste, Via Licio Giorgieri 1, 34127 Trieste, Italy

Supporting Information

ABSTRACT: The mononuclear copper(II) complex $[\text{Cu}(\text{H}_2\text{L}^1)_2(\text{H}_2\text{O})](\text{ClO}_4)_2$ (**1**) (where $\text{H}_2\text{L}^1 = 1,10$ -phenanthroline-5,6-dioxime) reacts with copper(II) perchlorate in acetonitrile at ambient conditions in the presence of triethylamine to afford a copper(II) complex, $[\text{Cu}(\text{L}^3)_2(\text{H}_2\text{O})](\text{ClO}_4)_2$ (**2a**), of 1,10-phenanthroline furoxan. A similar complex $[\text{Cu}(\text{L}^3)_2\text{Cl}](\text{ClO}_4)$ (**2**) is isolated from the reaction of H_2L^1 with copper(II) chloride, triethylamine, and sodium perchlorate in acetonitrile. The two-



electron oxidation of the *vic*-dioxime to furoxan is confirmed from the X-ray single crystal structure of **2**. An intermediate species, showing an absorption band at 608 nm, is observed at $-20\text{ }^\circ\text{C}$ during the conversion of **1** to **2a**. A similar blue intermediate is formed during the reaction of $[\text{Cu}(\text{HDMG})_2]$ ($\text{H}_2\text{DMG} = \text{dimethylglyoxime}$) with ceric ammonium nitrate, but H_2DMG treated with ceric ammonium nitrate does not form any intermediate. This suggests the involvement of a copper(II) complex in the intermediate step. The intermediate species is also observed during the two-electron oxidation of other *vic*-dioximes. On the basis of the spectroscopic evidence and the nature of the final products, the intermediate is proposed to be a mononuclear copper(II) complex ligated by a *vic*-dioxime and a dinitrosoalkene. The dinitrosoalkene is generated upon two-electron oxidation of the dioxime. The transient blue color of the dioxime-copper(II)-dinitrosoalkene complex may be attributed to the ligand-to-ligand charge transfer transition. The intermediate species slowly decays to the corresponding two-electron oxidized form of *vic*-dioxime, i.e. furoxan and $[\text{Cu}(\text{CH}_3\text{CN})_4](\text{ClO}_4)$. The formation of two isomeric furoxans derived from the reaction of an asymmetric *vic*-dioxime, hexane-2,3-dioxime, and copper(II) perchlorate supports the involvement of a dinitrosoalkene species in the intermediate step. In addition, the oxidation of 2,9-dimethyl-1,10-phenanthroline-5,6-dioxime (H_2L^2) to the corresponding furoxan and subsequent formation of a copper(I) complex $[\text{Cu}(\text{L}^4)_2](\text{ClO}_4)$ (**3**) (where $\text{L}^4 = 2,9$ -dimethyl-1,10-phenanthroline furoxan) are discussed.

INTRODUCTION

Furoxans (1,2,5-oxadiazole-2-oxides) and benzofuroxans are important heterocycles for their potential NO donor¹ activity with wide application in biological, medicinal, and synthetic chemistry.^{1–10} The five-membered heterocyclic rings are formed by two-electron oxidative cyclization of *vic*-dioximes. A large number of oxidizing agents like hypohalite, ferricyanide, ceric ions, nitrogen oxides, manganese dioxide, and lead tetraacetate have been used for oxidative transformation of *vic*-dioximes.^{11,12} Copper(II) perchlorate is known as a strong oxidizing agent with the redox potential of $\text{Cu}^{2+}/\text{Cu}^+$ in acetonitrile being 0.952 V versus SCE.¹³ The strong oxidizing nature of copper(II) perchlorate in acetonitrile has recently been documented in the oxidation of aromatic amines to generate amine radical cations.^{14–16} We have reported on the oxidation of *vic*-dioximes to the corresponding furoxans in high yield at ambient conditions mediated by copper(II) ions.¹⁷

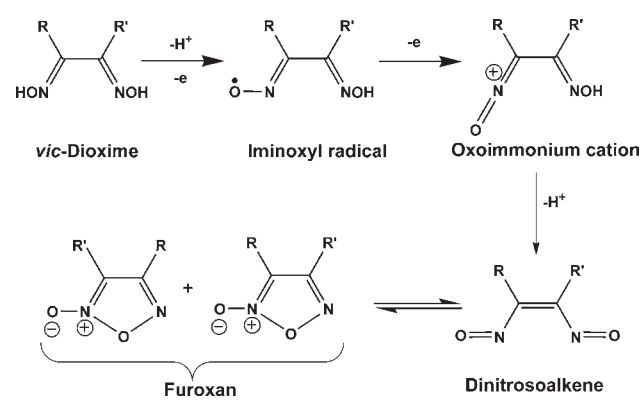
As a natural progression of our earlier work we have started investigating the mechanism of two-electron oxidation of *vic*-dioximes to furoxans. There are few examples where the involvement of iminoxyl radical species has been suggested during the

one-electron oxidation of monoximes.^{18–20} Low-temperature EPR study was reported for iminoxyl radical generated upon chemical oxidation of monooxime.^{21–24} In the electrochemical oxidation of *vic*-dioximes, a two-electron oxidized species, for example oxoimmonium cation via iminoxyl radical has been proposed that lead to the cyclized product.²⁵ Dinitrosoalkenes have been proposed as short-lived intermediates for the isomerization of unsymmetrical furoxans.^{26–28} The existence of an equilibrium between a furoxan ring and the corresponding dinitrosoalkene species has been established by trapping the latter with diene in a Diels–Alder reaction²⁹ and also by theoretical calculations.^{30,31} Direct evidence for the formation of dinitroso intermediate is available from IR and UV spectroscopic studies of photolysis product of either benzofuroxan or *o*-nitrophenyl azide in Ar matrices at 12–14 K.^{26,29,32,33} In course of investigating the mechanism of copper(II)-mediated oxidation reaction of dioxime to furoxan, we were interested to see if such

Received: May 10, 2011

Published: October 21, 2011

Scheme 1. Proposed Intermediate Species Involved during the Oxidation of *vic*-Dioxime to Furoxan



intermediate species could be stabilized via coordination with metal ion during the reaction. See Scheme 1.

As a result of our investigation we report herein the isolation and characterization of three five-coordinate copper(II) complexes, $[\text{Cu}(\text{H}_2\text{L}^1)_2(\text{H}_2\text{O})](\text{ClO}_4)_2$ (**1**), $[\text{Cu}(\text{L}^3)_2\text{Cl}](\text{ClO}_4)$ (**2**), and $[\text{Cu}(\text{L}^3)_2(\text{H}_2\text{O})](\text{ClO}_4)_2$ (**2a**), where L^1 is 1,10-phenanthroline-5,6-dioxime and L^3 is the corresponding furoxan derivative (Chart 1). We also report the oxidation of a new dioxime, 2,9-dimethyl-1,10-phenanthroline-5,6-dioxime (H_2L^2), to the corresponding furoxan along with the structural characterization of a copper(I)-phenanthroline furoxan complex, $[\text{Cu}(\text{L}^4)_2](\text{ClO}_4)$ (**3**). In exploring the mechanism of copper(II)-mediated oxidative reaction of *vic*-dioximes, we have observed a transient blue intermediate. A ternary copper(II) complex of dioxime and dinitrosoalkene ligands is proposed to be the intermediate species. These intriguing results along with the role of metal ion and solvent in the oxidation reaction are discussed.

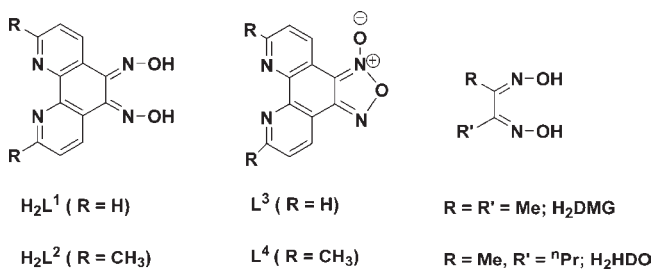
EXPERIMENTAL SECTION

Commercial grade chemicals were used for the synthetic purposes. Solvents were distilled and dried before use. *Although no problems were encountered during the synthesis of the complexes, perchlorate salts are potentially explosive and should be handled with care!*³⁴ 1,10-phenanthroline-5,6-dioxime (H_2L^1)³⁵ and $[\text{Cu}(\text{HDMG})_2]$ ³⁶ were synthesized according to literature procedures. The synthesis and characterization of $[\text{Cu}(\text{L}^3)_2\text{Cl}](\text{ClO}_4)$ (**2**) and isolation of L^3 from **2** has been reported earlier by our group.¹⁷ 2,9-Dimethyl-1,10-phenanthroline-5,6-dione was prepared according to a modification of the procedure described in the literature.^{37,38}

Fourier transform infrared spectroscopy on KBr pellets was performed on a Shimadzu FTIR 8400S instrument. Elemental analyses were performed on a PerkinElmer 2400 series II CHN analyzer. Electrospray ionization mass spectra were recorded with a Waters QTOF Micro YA263. ¹H NMR spectra were measured at room temperature using Bruker DPX-300 and 500 MHz NMR spectrometer. Solution electronic spectra were recorded on a HP8453 diode-array spectrometer with samples maintained at low temperature using a cryostat from Unisoku Scientific Instruments, Osaka, Japan. X-band EPR measurements were performed on a JEOL JES-FA 200 instrument.

Synthesis. 2,9-Dimethyl-1,10-phenanthroline-5,6-dioxime (H_2L^2). A mixture of 2,9-dimethyl-1,10-phenanthroline-5,6-dione (0.22 g, 0.92 mmol), $\text{NH}_2\text{OH} \cdot \text{HCl}$ (0.25 g, 3.69 mmol), and BaCO_3 (0.73 g, 3.71 mmol) was dissolved in 30 mL ethanol and the solution was allowed to reflux with

Chart 1. Ligands



stirring for 12 h. The solution was then cooled to room temperature and the solvent was removed under reduced pressure to obtain a yellow solid. The solid was suspended in 20 mL 4.2(N) dilute HCl solution and stirred vigorously for 4–5 h to precipitate a light-yellow solid. The solid was washed with ice-cold water, diethyl ether, and finally with dichloromethane. Yield: 0.10 g (40%). Anal. Calcd for $\text{C}_{14}\text{H}_{12}\text{N}_4\text{O}_2 \cdot 0.5\text{CH}_2\text{Cl}_2$ (310.73 g/mol): C, 56.05; H, 4.22; N, 18.03. Found: C, 56.10; H, 4.12; N, 17.48. IR (KBr, cm^{-1}): 3394(vs), 3086(w), 2669–2607(m), 1629(vs), 1587(m), 1523(m), 1423(s), 1383(s), 1352(w), 1294(w), 1138(m), 1101(m), 1053(s), 1016(s), 839(s), 804(s), 686, 586. ESI-MS (positive ion mode, $\text{MeCN}-\text{H}_2\text{O}$): $m/z = 291.40$ (22%, $[\text{H}_2\text{L}^2+\text{Na}]^+$), 269.39 (100%, $[\text{H}_2\text{L}^2+\text{H}]^+$). ¹H NMR [$(\text{CD}_3)_2\text{SO}$, 300 MHz, 25 °C]: δ , ppm: (13.31(br) and 12.83(br), 2H), (9.07 (d, $J = 8.2$ Hz) and 8.98 (d, $J = 8.2$ Hz), 1H), (8.46 (d, $J = 8.2$ Hz) and 8.33 (d, $J = 8.0$ Hz), 1H) 7.66–7.60(m, 2H), 5.75 (due to CH_2Cl_2), 2.75–2.72 (m, 6H).

$[\text{Cu}(\text{H}_2\text{L}^1)_2(\text{H}_2\text{O})](\text{ClO}_4)_2$ (**1**). To a suspension of H_2L^1 (0.72 g, 3 mmol) in 25 mL acetonitrile, $\text{Cu}(\text{ClO}_4)_2 \cdot 6\text{H}_2\text{O}$ (0.55 g, 1.5 mmol) was added and the mixture was allowed to stir for 12 h under ambient condition to precipitate a deep-green solid. The solid was isolated by filtration and the filtrate was kept for slow evaporation of solvent. X-ray quality single crystals of **1** were obtained from the green filtrate. Yield: 0.76 g (66%). Anal. Calcd for $\text{C}_{24}\text{H}_{18}\text{Cl}_2\text{CuN}_8\text{O}_{13}$ (760.90 g/mol): C, 37.88; H, 2.38; N, 14.73. Found: C, 38.28; H, 2.30; N, 14.91. IR (KBr, cm^{-1}): 3431(br), 3157(w), 3103(w), 2925(w), 1622(w), 1579(m), 1500(m), 1466(w), 1411(s), 1117(vs), 1403(s), 1001(m), 923(w), 818(m), 729(m), 627(s). ESI-MS (positive ion mode, MeCN): $m/z = 643.05$ (8%, $[(\text{H}_2\text{L}^1)_2\text{Cu}+\text{ClO}_4]^+$), 543.09 (70%, $[(\text{H}_2\text{L}^1)_2\text{Cu}]^+$), 525.08 (32%, $[(\text{H}_2\text{L}^1)_2\text{Cu}-\text{H}_2\text{O}]^+$), 272.05 (22%, $[(\text{H}_2\text{L}^1)_2\text{Cu}]^{2+}$), 241.08 (100%, $[\text{H}_2\text{L}^1+\text{H}]^+$), 223.07 (10%, $[(\text{H}_2\text{L}^1-\text{H}_2\text{O})+\text{H}]^+$). UV–vis in MeCN : λ , nm (ϵ , $\text{M}^{-1}\text{cm}^{-1}$): 905 (sh), 675 (130), 465 (sh), 338 (13,700).

$[\text{Cu}(\text{L}^3)_2(\text{H}_2\text{O})](\text{ClO}_4)_2$ (**2a**). To a suspension of H_2L^1 (0.24 g, 1 mmol) in 20 mL acetonitrile was added a solution of $\text{Cu}(\text{ClO}_4)_2 \cdot 6\text{H}_2\text{O}$ (0.92 g, 2.5 mmol). Triethyl amine (0.276 mL, 2 mmol) was added to that mixture and was allowed to stir for 12 h at room temperature. A green solid was precipitated from the green solution. The solid was isolated by filtration and dried. Another batch of **2a** was obtained by slow evaporation of the filtrate. Yield: 0.18 g (47%). Anal. Calcd for $\text{C}_{24}\text{H}_{14}\text{Cl}_2\text{CuN}_8\text{O}_{13}$ (756.87 g/mol): C, 38.09; H, 1.86; N, 14.80. Found: C, 38.10; H, 1.92; N, 15.03. IR (KBr, cm^{-1}): 3448(w), 3356(w), 3076(w), 2924(w), 1633(m), 1591(m), 1506(m), 1456(w), 1411(m), 1143–1086(vs), 821(m), 727(m), 628(m). ESI-MS (positive ion mode, MeCN): $m/z = 538.97$ (100%, $[(\text{L}^3)_2\text{Cu}]^+$), 300.95 (75%, $[\text{L}^3\text{Cu}]^+$). UV–vis in MeCN (λ , nm; ϵ , $\text{M}^{-1}\text{cm}^{-1}$): 700 (292), 330 (11,000).

$[\text{Cu}(\text{L}^4)_2](\text{ClO}_4)$ (**3**). The dioxime ligand H_2L^2 (0.18 g, 0.67 mmol) was treated with $\text{Cu}(\text{ClO}_4)_2 \cdot 6\text{H}_2\text{O}$ (0.50 g, 1.34 mmol) in acetonitrile. The solution was allowed to stir at room temperature for 1 d to yield a dark red solution. The solution was kept for slow evaporation of solvent to isolate red needle shaped crystals for X-ray diffraction. Yield: 0.14 g

Table 1. Crystallographic Data for Complexes 1, 2, and 3

	1	2·0.5(H ₂ O)	3·CH ₃ CN
empirical formula	C ₂₄ H ₁₈ Cl ₂ CuN ₈ O ₁₃	C ₂₄ H ₁₃ Cl ₂ CuN ₈ O _{8.5}	C ₃₀ H ₂₃ ClCuN ₉ O ₈
fw	760.90	683.86	736.56
cryst syst	monoclinic	monoclinic	triclinic
space group	<i>P</i> 2 ₁ / <i>n</i>	<i>P</i> 2 ₁ / <i>c</i>	$\bar{P}1$
<i>a</i> /Å	13.439(2)	13.127(3)	8.907(2)
<i>b</i> /Å	13.926(2)	15.606(4)	10.053(3)
<i>c</i> /Å	15.375(2)	25.530(5)	17.151(3)
α /°	90.00	90.00	83.664(10)
β /°	108.848(2)	95.04(3)	80.11(2)
γ /°	90.00	90.00	83.203(10)
volume/Å ³	2723.3(6)	5210(2)	1496.0(6)
<i>Z</i>	4	8	2
<i>D</i> _{calc} /gcm ⁻³	1.856	1.744	1.635
μ MoK α /mm ⁻¹	1.087	1.114	0.890
<i>F</i> (000)	1540	2752	752
θ range, deg	1.75–22.52	2.03–26.36	1.21–21.66
no. of reflns colld	21 053	55 335	10 292
no. of indep reflns	3402	10 318	3519
<i>R</i> _{int}	0.0450	0.0669	0.0940
no. of reflns (<i>I</i> > 2 σ (<i>I</i>))	2201	4397	2243
no. of refined params	456	784	502
goodness-of-fit (<i>F</i> ²)	1.018	0.817	1.051
<i>R</i> ₁ , <i>wR</i> ₂ (<i>I</i> > 2 σ (<i>I</i>)) ^a	0.0680, 0.1573	0.0524, 0.1309	0.0774, 0.2151
<i>R</i> ₁ , <i>wR</i> ₂ (all data) ^a	0.1115, 0.1841	0.1254, 0.1531	0.1154, 0.2420
residuals, e/Å ³	0.642, -0.521	0.783, -0.582	1.949, ^b -0.792

^a $R_1 = \sum ||F_o| - |F_c|| / \sum |F_o|$, $wR_2 = [\sum w (F_o^2 - F_c^2)^2 / \sum w (F_o^2)^2]^{1/2}$. ^b Close to a perchlorate anions having high thermal motion

(60%). Anal. Calcd for C₂₈H₂₀ClCuN₈O₈ (695.51 g/mol): C, 48.35; H, 2.90; N, 16.11. Found: C, 48.21; H, 2.91; N, 16.12. IR (KBr, cm⁻¹): 3433(br), 3076(w), 2924(w), 1632(s), 1583(m), 1526(m), 1487–1442(w), 1383(m), 1140–1091(vs), 993(w), 838(m). ESI-MS (positive ion mode, MeCN): *m/z* = 329.03 (5%, [(L⁴)Cu]⁺), 289.09 (30%, [L⁴+Na]⁺), 267.12 (100%, [L⁴+H]⁺). UV–vis in MeCN (λ , nm; ϵ , M⁻¹cm⁻¹): 458 (456), 332 (sh). ¹H NMR [(CD₃)₂SO, 500 MHz, 25 °C], δ , ppm: 9.09 (d, 1H, *J* = 8.0 Hz), 8.96 (d, 1H, *J* = 8.5 Hz), 8.10–8.06 (m, 2H), 2.42 (s, 3H), 2.39 (s, 3H).

Isolation of L⁴. The red solution obtained after the reaction of H₂L² (0.07 g, 0.27 mmol) with Cu(ClO₄)₂·6H₂O (0.40 g, 1.08 mmol) in acetonitrile was evaporated to dryness by a rotary evaporator and was treated with 100 mL aq. NH₃. The mixture was stirred for 3 h to get a clear green solution. The organic product was extracted with dichloromethane. The organic layer was dried over anhydrous Na₂SO₄ and removal of solvent gave an off-white solid of L⁴. Yield: 0.05 g (68%). Anal. Calcd for C₁₄H₁₀N₄O₂·0.5H₂O (275.25 g/mol): C, 61.09; H, 4.03; N, 20.35. Found: C, 61.35; H, 4.04; N, 19.51. IR (KBr, cm⁻¹): 3470(br), 2958–2852(m), 1627(s), 1587(s), 1521(s), 1489(s), 1440(m), 1379(s), 1261(w), 1134(w), 1072(w), 983(w), 833(m), 798, 748, 615. ESI-MS (positive ion mode, MeCN): *m/z* = 289.10 (100%, [L⁴+Na]⁺), 267.12 (40%, [L⁴+H]⁺). ¹H NMR [(CD₃)₂SO, 300 MHz, 25 °C]: δ , ppm: 8.69–8.63 (m, 2H), 7.73–7.69 (m, 2H), 2.77 (s, 3H), 2.75 (s, 3H). ¹³C NMR [(CD₃)₂SO, 125 MHz, 25 °C]: δ , ppm: 163.25, 161.56, 150.15, 147.94, 146.77, 132.36, 131.13, 125.48, 125.16, 116.90, 114.14, 108.65, 25.66, 25.54.

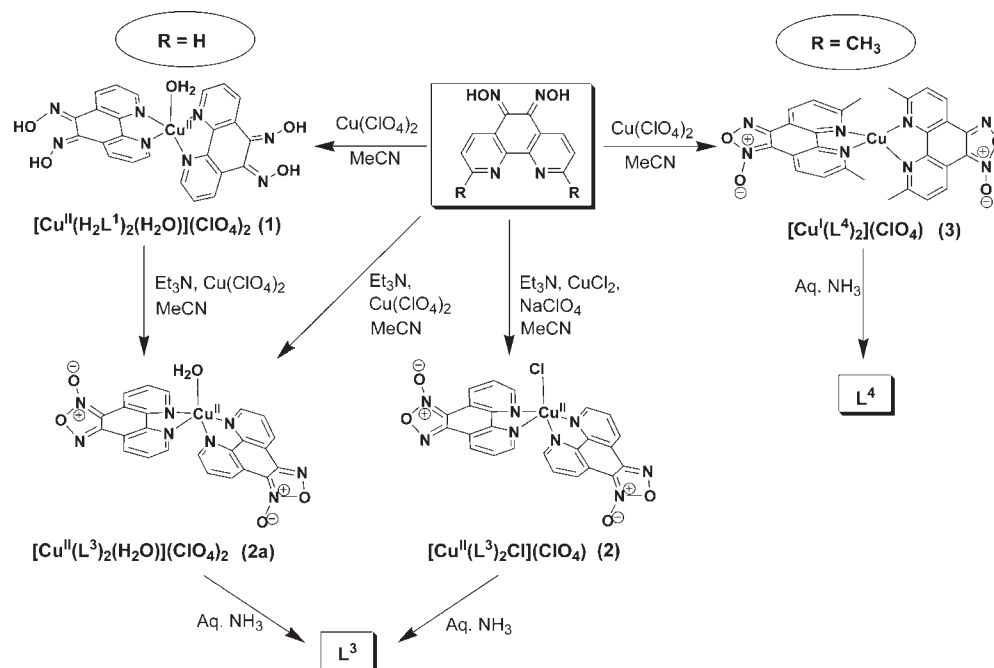
X-ray Crystallographic Data Collection and Refinement of the Structures. Crystallographic data for 1, 2, and 3 are given in Table 1. Diffraction data for all compounds were collected at room temperature with Mo–K α radiation (λ = 0.71073 Å). Diffraction data

for 1 and 3 were collected on a Bruker Smart APEX II, whereas the experiment for 2 was performed on a Nonius DIP-1030H system. Cell refinement, indexing and scaling of all of the data sets were carried out using the *ApeX2 v2.1-0* software (for 1 and 3),³⁹ and packages *Denzo* and *Scapecap* for 2.⁴⁰ All the structures were solved by direct methods and subsequent Fourier analyses and refined by the full-matrix least-squares method based on *F*² with all observed reflections.⁴¹ H atoms were placed at calculated positions, those of oxime groups in 1 were fixed with AFIX 147 instruction of SHELXL (O–H distance of 0.82 Å). A perchlorate anion in 1 was found to be disordered over two positions (refined occupancies 0.80(2) and 0.20(2)) about a Cl–O bond and a residual in 2 was interpreted as a lattice water molecule (H atoms not assigned). Compound 3, which crystallizes with an acetonitrile molecule, has one of the phenanthroline furoxan ligand disordered over two coplanar orientations (refined occupancies 0.69(2)/0.31(2)). The atoms at lower occupancy in all the disorder situations were isotropically refined. ORTEP drawings (40% probability ellipsoids) were prepared with program *Cameron*⁴² included in the WinGX System, Ver 1.80.05.⁴³ The low theta value is a consequence of low diffracting crystals for 1 and 3 and of the highly disordered ligand detected in 3.

RESULTS AND DISCUSSION

Synthesis and Characterization. 1,10-Phenanthroline-5,6-dioxime (H₂L¹) was synthesized according to a literature procedure.³⁵ 2,9-Dimethyl-1,10-phenanthroline-5,6-dioxime (H₂L²) was synthesized by a modification of the procedure for the synthesis of H₂L¹. ESI-MS of H₂L² shows ion peaks at *m/z* = 291.40 (22%) and 269.39 (100%) with expected isotope

Scheme 2. Synthesis of Copper Complexes



distribution patterns calculated for $[H_2L^2+Na]^+$ and $[H_2L^2+H]^+$, respectively. 1H NMR spectrum of H_2L^2 exhibits two broad peaks at 13.31 and 12.83 ppm due to the oxime groups. Additionally, the number of resonances for aromatic protons is found to be more than the precursor dione compound. A set of five resonances for aromatic protons are observed the region 7.60–9.09 ppm. However, the integration ratio for methyl:aromatic:oxime protons of 6:4:2 is consistent with the dioxime ligand. A higher number of proton resonances suggest the presence of an isomerization equilibrium owing to the intramolecular hydrogen-bonding interactions between the two oxime groups in H_2L^2 . $[Cu(H_2L^1)_2(H_2O)](ClO_4)_2$ (**1**) (Scheme 2) was prepared by reacting H_2L^1 with copper(II) perchlorate in acetonitrile in the absence of any base. While complex $[Cu(L^3)_2Cl](ClO_4)$ (**2**) was isolated from the reaction of H_2L^1 , $CuCl_2$ and $NaClO_4$ in the presence of triethylamine, complex $[Cu(L^3)_2(H_2O)](ClO_4)_2$ (**2a**) was synthesized using H_2L^1 , triethylamine, and $Cu(ClO_4)_2$ in acetonitrile. The mononuclear copper(I) complex $[Cu(L^4)_2](ClO_4)$ (**3**) was isolated by treating the sterically hindered phenanthroline-based ligand H_2L^2 with copper(II) perchlorate under air at room temperature in acetonitrile. In the reaction, ligand H_2L^2 gets oxidized to L^4 and copper(II) is reduced to copper(I) with subsequent formation of the copper(I) complex (**3**). It is important to mention here that the formation of copper(I) complex was not observed with other furoxan ligands. The phenanthroline furoxan ligands L^3 and L^4 were isolated from the complexes using aqueous ammonia solution (Scheme 2). ESI-MS in positive ion mode (in acetonitrile) of the new furoxan ligand L^4 shows ion peaks at $m/z = 289.10$ (100%) and 267.12 (40%) with expected isotope distribution patterns calculated for $[L^4+Na]^+$ and $[L^4+H]^+$, respectively. 1H NMR spectrum of L^4 in $DMSO-d_6$ does not show any oxime–OH peaks in the region 12–14 ppm as observed in H_2L^2 . However, four aromatic

protons of the phenanthroline backbone are observed in the region 7.69–8.69 ppm and the peak positions and splitting patterns are considerably different from that in H_2L^2 . All other compounds were also characterized by different spectroscopic and analytical techniques. Additionally, the copper complexes (**1**, **2**, and **3**) were structurally characterized by single-crystal X-ray diffraction.

The crystallographic independent unit of $[Cu(H_2L^1)_2(H_2O)](ClO_4)_2$ (**1**) comprises of a dicationic mononuclear five-coordinate copper(II) complex (Figure 1) and perchlorate counterions. The geometry around the copper ion can be described as distorted trigonal bipyramidal ($\tau = 0.55$)⁴⁴ with the metal center coordinated by two neutral dioxime H_2L^1 ligands and a water molecule. The nitrogen donors N2 and N4 from different phenanthrolines and the oxygen atom (O5) of the aqua ligand form the equatorial plane, whereas the remaining nitrogen donors N1 and N3 coordinate at the apical positions with the N(1)–Cu(1)–N(3) angle of $170.3(3)^\circ$ (Table 2). The Cu–N bond distances in the equatorial plane (2.015(7), 2.072(6) Å) are longer than the apical ones (1.953(7), 1.972(7) Å), whereas the Cu–OH₂ distance of 2.164(8) Å is consistent with values found in the nitrate and perchlorate $[Cu(H_2O)(1,10\text{-phenanthroline})_2]^{2+}$ derivatives.^{45,46} The phenanthroline mean planes in **1** form a dihedral angle of $57.08(11)^\circ$.

All the oxime fragments are coplanar with the phenanthroline plane with N–O bond distances that range from 1.347(9) to 1.379(9) Å. These groups are involved in intramolecular hydrogen bonding interactions (average $N \cdots O$ distance of 2.50 Å). In addition, an intermolecular H-bonding interaction is observed to occur between the oxime groups O(1)–H and O(4)–H with perchlorate oxygens (2.72 Å), while the aqua ligand connects O(3) (2.80 Å, at $-x + 2, -y + 1, -z + 1$) and a perchlorate oxygen (2.71 Å) to form a 2D polymeric layer parallel to the bc plane (Figure S1 of the Supporting Information).

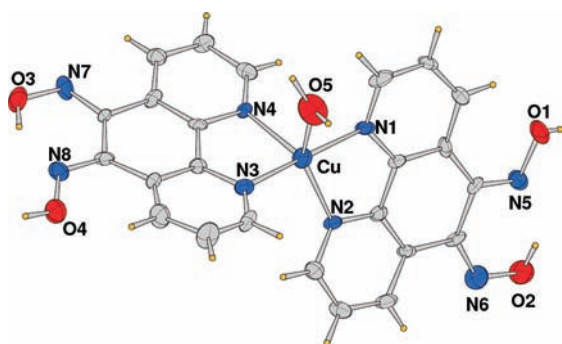


Figure 1. ORTEP drawing of the molecular cation of $[\text{Cu}(\text{H}_2\text{L}^1)_2\text{-(H}_2\text{O)}](\text{ClO}_4)_2$ (**1**).

Table 2. Selected Bond Lengths (Å) and Angles (°) for **1**, **2**, and **3**

	1, X = O(5)		2, X = Cl(1)		3 ^a
	Mol A	Mol B	Mol A	Mol B	
Cu–N(1)	1.953(7)	2.004(4)	1.996(4)	2.057(12)	
Cu–N(2)	2.015(7)	2.034(4)	2.053(4)	1.932(13)	
Cu–N(3)	1.972(7)	2.013(4)	1.997(4)	2.034(7)	
Cu–N(4)	2.072(6)	2.206(4)	2.181(5)	2.025(7)	
Cu–X	2.164(8)	2.2759(16)	2.2928(15)		
N(5)–O(1)	1.370(8)	1.378(7)	1.358(7)	1.35(2)	
N(6)–O(1)		1.461(6)	1.452(8)	1.48(3)	
N(6)–O(2)	1.347(9)	1.239(6)	1.198(7)	1.21(2)	
N(7)–O(3)	1.351(8)	1.369(6)	1.243(9)	1.380(10)	
N(8)–O(3)		1.430(7)	1.363(10)	1.436(11)	
N(8)–O(4)	1.379(9)	1.190(6)	1.101(9)	1.223(10)	
N(1)–Cu–N(2)	82.4(3)	81.22(17)	81.02(17)	82.1(7)	
N(3)–Cu–N(4)	81.2(3)	78.39(16)	79.6(2)	81.4(3)	
N(1)–Cu–N(3)	170.3(3)	174.65(18)	174.71(18)	123.7(5)	
N(1)–Cu–N(4)	104.4(3)	103.69(16)	99.36(18)	113.8(5)	
N(2)–Cu–N(3)	99.9(3)	93.61(16)	94.13(18)	122.0(5)	
N(2)–Cu–N(4)	131.4(3)	99.04(16)	103.20(17)	139.5(5)	
N(1)–Cu–X	87.1(3)	95.15(13)	95.98(13)		
N(2)–Cu–X	137.6(3)	163.37(13)	155.85(13)		
N(3)–Cu–X	84.8(3)	89.42(12)	89.30(13)		
N(4)–Cu–X	91.0(3)	97.58(12)	100.94(12)		

^aData relative to the disordered phenanthroline at higher occupancy only.

The X-ray crystal structure of the monocationic complex $[\text{Cu}(\text{L}^3)_2\text{Cl}](\text{ClO}_4)$ (**2**) reveals two crystallographic independent complexes (A, B) comprising of five-coordinate copper(II) ion. At first sight the complex appears similar to **1**, being the metal ion bischelated by the neutral furoxan (L^3) ligands and by a chloride. However, in the present case the analysis of bond angles indicates a coordination geometry, which can be described as distorted square-pyramidal ($\tau = 0.19$ and 0.31 , for molecules A and B, respectively). The molecular cation A with atom labeling scheme is depicted in Figure 2, where the N(1), N(2), and N(3) phenanthroline nitrogen donors and the chloro ligand are located in the basal plane, while N(4) occupies the apical position.

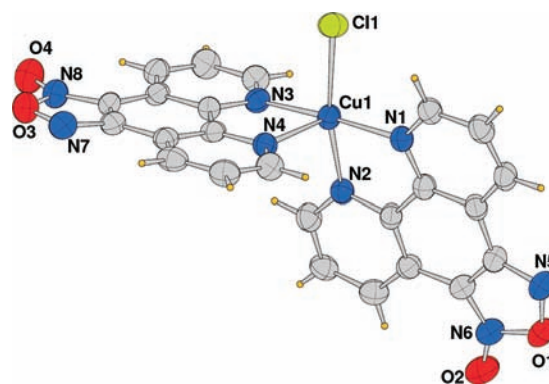


Figure 2. ORTEP drawing of one of the two independent molecular cations of $[\text{Cu}(\text{L}^3)_2\text{Cl}](\text{ClO}_4)$ (**2**).

The Cu–N bonds in the base of the pyramid fall within 1.996(4)–2.053(4) Å, whereas the apical nitrogen is positioned at significant longer distance, of 2.206(4) and 2.181(5) Å respectively in the two independent complexes. The Cu–Cl bond length is 2.276(2) Å in complex A and 2.293(1) Å in B, which are within the range measured in $[\text{CuCl}(1,10\text{-phenanthroline})_2]^+$ complex cation,⁴⁷ and slight differences can be attributed to the packing and the different coordination geometry. In addition, the Cu–N bond, located trans to the chloro ligand, is slightly longer than the other values in the basal plane. The angles N(1)–Cu(1)–N(3) and N(2)–Cu(1)–Cl(1) (174.65(18) and 163.37(13)°, respectively) are clearly indicative of the distortions about the metal center, while the corresponding values in molecule B are 174.71(18) and 155.85(13)°, respectively (Table 2). The L^3 ligands have coplanar atoms and the phenanthroline planes form a dihedral angle of 74.46(7) and 66.39(7)° in each complex. A residual in the difference Fourier map was assigned to a water oxygen located at H-bond distance from a perchlorate oxygen and from O(4) of the furoxan moiety (Ow...O distances of 2.77 and 2.95 Å, respectively). The crystal packing does not show any significant π – π stacking interaction among aromatic rings of the complexes.

The X-ray structural analysis of **2** confirms the oxidative transformation of the phenanthroline dioxime ligand to form a five-membered furoxan ring fused at positions 5,6 of the phenanthroline. The N(5)–O(1), N(6)–O(1) and N(6)–O(2) bond distances of 1.337(7), 1.427(8) and 1.182(7) Å (mean values of four fragments), respectively, are in agreement with those measured in the crystallographically characterized 4,7-dichloro- and 4,7-dibromobenzo[*c*]furoxan-1-oxide compound.⁴⁸

Attempts to crystallize the aqua derivative **2a** were unsuccessful. However, it is likely that this complex could have a coordination geometry similar to that of **2** with a coordinated water replacing the chloride at the fifth coordination site.

The X-ray structure of the monocationic complex, $[\text{Cu}(\text{L}^4)_2](\text{ClO}_4)$ (**3**), reveals the copper ion in a highly distorted tetrahedral coordination geometry, being chelated by two 2,9-dimethyl-1,10-phenanthroline furoxan ligands (L^4). The phenanthroline furoxan ligands are almost perpendicular to each other forming a dihedral angle of 73.06(16)°. The complex geometry is typical of copper(I) ion but the tetrahedral arrangement is also assumed to alleviate the mutual steric interaction of the methyl groups at 2,9 positions of the phenanthroline. Ligand L^4 is formed upon oxidation of dioxime H_2L^2 where copper(II) is reduced to copper(I) with subsequent formation of the copper(I) complex (**3**).

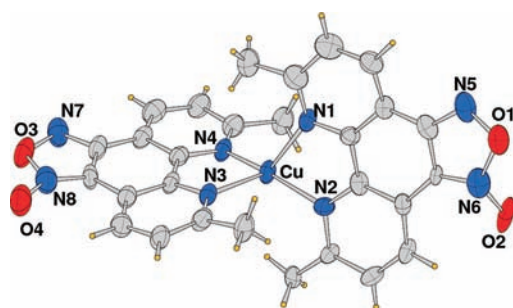


Figure 3. ORTEP drawing of the cation of $[\text{Cu}(\text{L}^4)_2](\text{ClO}_4)$ (**3**). The phenanthroline furoxan ligand N1/N2 is disordered over two contiguous coplanar orientations, only that at higher occupancy (69%) is shown.

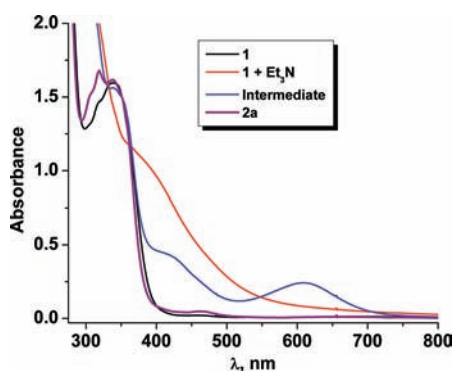


Figure 4. Optical spectra of **1** (0.1 mM), **1** with triethylamine, **2a**, and the intermediate species in acetonitrile at room temperature during the conversion of **1** to **2a**.

The Cu–N bond distances, in a range from 1.932(13) to 2.057(12) Å, are comparable within their e.s.d.'s with those measured in the other complexes here presented despite the different coordination geometry and metal oxidation state. As described in the Experimental section, the N1/N2 phenanthroline furoxan ligand is disordered over two coplanar orientations, which seems determined to favor π – π interactions between the furoxan fragment and phenanthroline rings of symmetry related complexes (distance between centroid rings of ca. 3.45 Å) See Figure 3.

Mechanistic Studies on the Oxidation of 1,2-Dioximes to Furoxans. As stated previously, the formation of copper(II)-phenanthroline furoxan complex (**2a**) takes place by reacting H_2L^1 with a little excess of copper(II)-perchlorate in acetonitrile under ambient conditions in the presence of triethylamine. Complex **1**, on the other hand, reacts with four equivalents of copper(II)-perchlorate and two equivalents of triethylamine to afford **2a**. Therefore, the base plays an important role in the transformation reaction. The oxidation of dioxime to furoxan involves two electrons with concomitant change in proton content. The presence of a base facilitates the reaction by accepting the oxime protons of H_2L^1 . The conversion of **1** to **2a** was monitored spectrophotometrically to understand the reaction pathway. An acetonitrile solution of **1**, when treated with 2 equivalents of triethylamine, results in a change in the oxime-to-metal charge transfer band, indicating the formation of a copper(II)-phenanthroline oximate complex. The resulting solution upon treatment with four equivalents of $\text{Cu}(\text{ClO}_4)_2 \cdot 6\text{H}_2\text{O}$ turns to a deep-blue species with the λ_{max} at 608 nm (Figure 4).

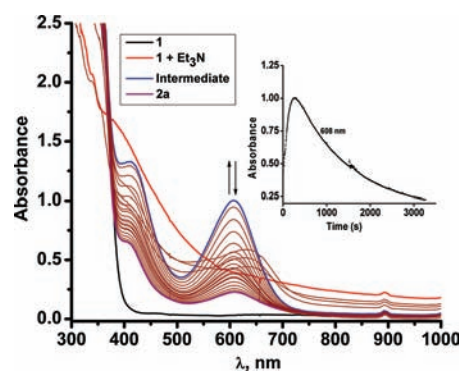


Figure 5. Optical spectral changes during the conversion of **1** (0.25 mM) to **2a** in the presence of triethylamine and copper(II) perchlorate at -20°C in acetonitrile.

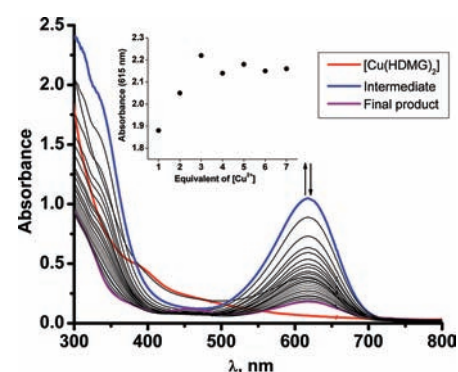


Figure 6. Optical spectral changes during the reaction of $[\text{Cu}(\text{HDMG})_2]$ (0.25 mM) with copper(II) perchlorate at -20°C in acetonitrile. Inset: Dependence of Cu^{2+} concentration on the formation of intermediate species.

Interestingly, the blue species rapidly decays to a light green solution; the optical spectrum of the solution does match with that of the independently prepared **2a**. ESI-MS of the final green solution confirms the oxidation of oxime H_2L^1 to L^3 . The blue species is therefore an intermediate in the oxidation of oxime to furoxan. However, the formation and decay of the transient intermediate could not be monitored at ambient conditions. The conversion of **1** to **2a** was, therefore, monitored spectrophotometrically at -20°C to observe the transient species at 608 nm. The intermediate species decays following a pseudo-first-order rate $k = 5.86 \times 10^{-4} \text{ s}^{-1}$ to **2a** (Figure 5). It is important to note that four equivalents of copper(II) perchlorate are needed for maximum formation of the intermediate species.

We have earlier reported the oxidation of a series of 1,2-dioximes using copper(II) perchlorate as the oxidant.¹⁷ To understand the nature of the intermediate species involved in the transformation reaction, we have performed the low-temperature kinetics using other *vic*-dioximes. A copper(II) complex of dimethylglyoxime, $[\text{Cu}(\text{HDMG})_2]$ was used for the reaction with copper(II) perchlorate in acetonitrile at -20°C . A similar transient blue intermediate species featuring a CT band at 615 nm was observed (Figure 6).

Here also, the transient intermediate forms very fast and decays following a pseudo-first-order rate $k = 2.29 \times 10^{-3} \text{ s}^{-1}$ (Figure 6). A set of copper(II) perchlorate solutions of variable concentration were mixed with 0.25 mM solution of $[\text{Cu}(\text{HDMG})_2]$ in

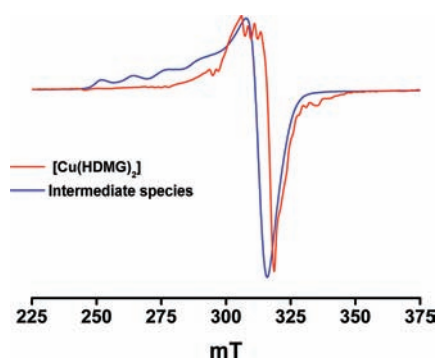


Figure 7. X-band EPR spectra of $[\text{Cu}(\text{HDMG})_2]$ and the intermediate species in frozen acetonitrile at 123 K.

acetonitrile and the formation and decay of the intermediate species were monitored optically at $-20\text{ }^\circ\text{C}$. It is found that the formation of blue species depends on the concentration of copper(II) perchlorate added and attains the maximum concentration in the presence of three equivalents of copper(II) salt (insert in Figure 6). The use of ceric ammonium nitrate as an oxidizing agent yields a similar chromophore at 615 nm, suggesting that neither a metal cluster nor an oxidized metal center is responsible for the CT band. Moreover, ceric ammonium nitrate or copper(II) perchlorate fails to carry out the oxidation in any solvent other than acetonitrile. Hence it proves that a combination of copper(II) salt and acetonitrile is important for the formation of the blue intermediate species and to carry out the oxidative transformation process. In addition, all the experiments were repeated under nitrogen atmosphere in a glovebox. The oxidation of *vic*-dioxime to furoxan under oxygen-free environment suggests that oxygen has no effect in the transformation reaction.

The same intermediate species is observed in the reaction of free H_2DMG with copper(II) perchlorate in acetonitrile at $-20\text{ }^\circ\text{C}$. Interestingly, treatment of *vic*-dioximes with ceric ammonium nitrate does not produce the intermediate species. This supports the intermediate to be a copper(II) complex. To understand the stoichiometry of metal and HDMG involved in electron transfer, the intermediate was monitored with a set of solutions with fixed concentration of copper(II) perchlorate by adding H_2DMG solution of variable concentration at $-40\text{ }^\circ\text{C}$. The experimental results indicate that the species is constituted of metal and HDMG in a 1:2 ratio as it attains the maximum absorbance after addition of two equivalents of H_2DMG and remains almost unchanged upon further addition. The rate of decay increases with an increase in the concentration sharply up to three equivalents of added copper(II) perchlorate solution. Then the decay rate remains almost unaltered upon further addition of copper(II) perchlorate solution.

The X-band EPR spectrum of the transient blue intermediate in a frozen solution at 123 K shows four line hyperfine splitting pattern arising from the g_{\parallel} region due to a mononuclear copper(II) species. The symmetry of the paramagnetic center is axial with $g_{\perp} = 2.07$, $g_{\parallel} = 2.39$, and $A_{\parallel} = 112 \times 10^{-4}\text{ cm}^{-1}$ (Figure 7). The $g_{\parallel}/A_{\parallel}$ value of 214 predicts a distorted tetrahedral geometry at the copper(II) center.⁴⁹ The EPR spectra of the intermediate species generated upon treatment of $[\text{Cu}(\text{HDMG})_2]$ with ceric ammonium nitrate or with 2 equivalents of copper(II) perchlorate are very similar. The nature of the EPR spectrum rules out the possibility of one-electron oxidation either on metal center or

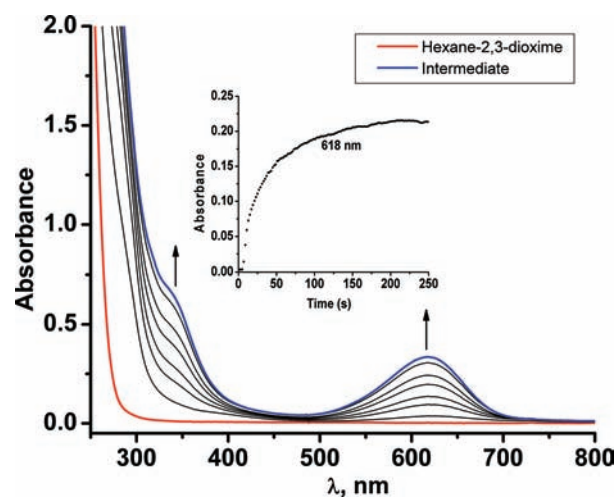


Figure 8. Optical spectral changes during the reaction of hexane-2,3-dioxime with 0.5 equivs of copper(II) perchlorate at $-20\text{ }^\circ\text{C}$ in acetonitrile.

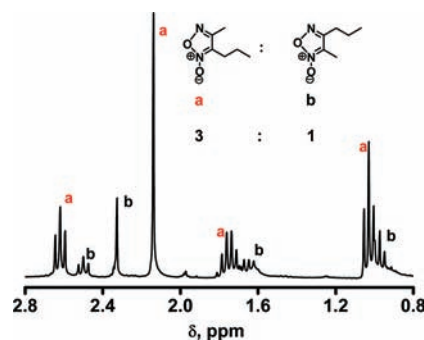
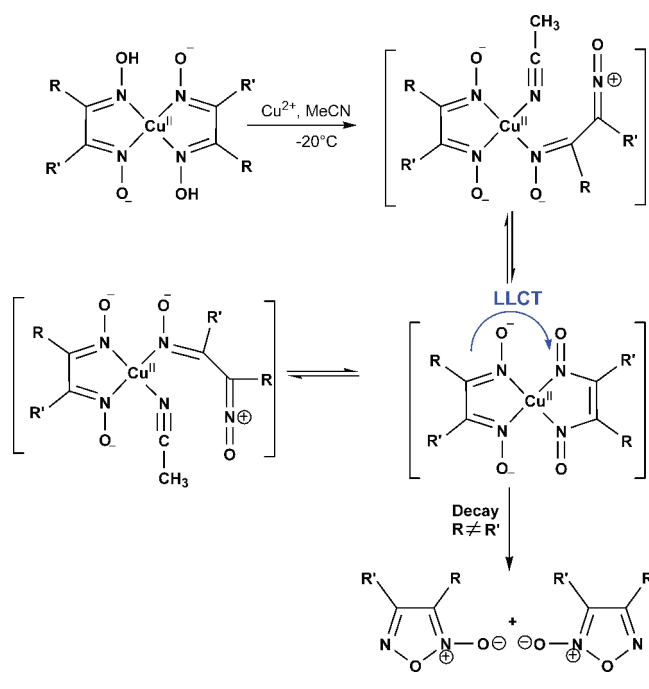


Figure 9. ^1H NMR spectrum of products derived from hexane-2,3-dioxime in CDCl_3 at $25\text{ }^\circ\text{C}$.

on the ligand. One-electron oxidation of $[\text{Cu}(\text{HDMG})_2]$ would result in the formation of a copper(II)-iminoxyl radical or copper(III) species. The EPR spectrum of the blue intermediate does not correspond to such species. The EPR parameters suggest a weaker equatorial bonding as a result of distortion from planarity. The blue intermediate is therefore an oxidized form of $[\text{Cu}(\text{HDMG})_2]$ where one of the dioximes gets oxidized by two electrons and weakens the equatorial bonding.

For hexane-2,3-dioxime the charge transfer transition is observed at 618 nm with a shoulder at 338 nm (Figure 8). The intermediate is formed with a pseudo-first-order rate of $3.22 \times 10^{-2}\text{ s}^{-1}$ and decays with a pseudo-first-order rate $k = 1.13 \times 10^{-2}\text{ s}^{-1}$. In this reaction, the ^1H NMR spectrum of the decay product after removal of metal ion reveals a 3:1 mixture of two isomeric furoxans (Figure 9). This is indicative of the formation of a transient species which cyclizes via two different pathways depending upon the stability of the transient intermediates.

The two-electron oxidation of the copper(II)-phenanthroline oxime complex may form either dinitrosoalkene or iminoxyl-diradical. To get an idea about the nature of the species the decay of the intermediate generated from $[\text{Cu}(\text{HDMG})_2]$ was monitored in the presence of different intercepting reagents. The presence of TEMPOH or 2,4,6-tri-*tert*-butylphenol do not

Scheme 3. Proposed Mechanism for the Oxidation of *vic*-Dioximes

affect the rate of decay of the blue intermediate and no signature of radical species is observed (Figures S2 and S3 of the Supporting Information). However, addition of 3,5-di-*tert*-butylcatechol enhances the rate of decay of the intermediate by 10 times and the formation of 3,5-di-*tert*-butylquinone is observed in the reaction solution (Figure S4 and Scheme S1 of the Supporting Information). Moreover, it has been reported that an iminoxyl radical derived from *vic*-dioxime gets easily oxidized by another electron than the oxime group.²⁵

On the basis of these results, the intermediate may be formulated as a mononuclear copper(II) complex coordinated by one oxime ligand and one two-electron oxidized form of the oxime, that is, a dinitroso or oxoimmonium cation. The blue color is observed due to the oxime-to-dinitroso charge transfer transition (Scheme 3). This type of LLCT have been observed in mixed ligand copper(II) complexes containing an electron rich bidentate donor and a bidentate acceptor ligand.⁵⁰ Simple dinitrosoalkenes are colorless and show no transition in the visible region.⁵¹ Examples of metal stabilized *vic*-dinitrosoalkanes in which both nitroso groups are coordinated to the same metal atom are known in the literature.^{52–57} However, there is no example of metal-coordinated dinitrosoalkene. The dioxime oxidation by copper(II) ions in acetonitrile reported in this work is proposed to occur via oxoimmonium cation/dinitroso species with concomitant formation of $[\text{Cu}(\text{CH}_3\text{CN})_4](\text{ClO}_4)$. It is important to note that the intermediate is observed only in acetonitrile and the ligand centered oxidation does take place in methanol or water.

The dinitrosoalkene or oxoimmonium cation may cyclize to give two different furoxans for unsymmetrical dioximes, whereas a single furoxan is isolated in case of symmetrical dioxime. The ratio of different furoxans obtained from unsymmetrical dioxime depends upon the nature of R and R' and relative stability of the intermediate species.

CONCLUSIONS

We have isolated and structurally characterized one mononuclear copper(II) and one mononuclear copper(I) complex of phenanthroline-based furoxan ligands. The ligands were derived from the corresponding copper(II)-phenanthroline dioxime complexes upon oxidation by copper(II)-perchlorate in acetonitrile. A dioxime-copper(II)-dinitrosoalkene species was proposed as transient intermediate involved in the two-electron oxidative transformation pathway. The intermediate was also observed during the oxidation of other *vic*-dioximes. The involvement of a dinitrosoalkene species in the reaction mechanism was further supported by the isolation of two isomeric furoxan from the oxidation of hexane-2,3-dioxime. The intermediate reported in this work is the first example of copper(II)-dinitrosoalkene species. The results discussed here demonstrate the role played by the metal ion in stabilizing the dinitrosoalkene species in the oxidative transformation reaction.

ASSOCIATED CONTENT

S Supporting Information. Crystallographic data in CIF file format, structure, and kinetic measurements. This material is available free of charge via the Internet at <http://pubs.acs.org>.

AUTHOR INFORMATION

Corresponding Author

*Fax: +91-33-2473-2805. Phone: +91-33-2473-4971. Email: ictkp@iacs.res.in.

ACKNOWLEDGMENT

We are grateful to the Department of Science and Technology (DST), Government of India for the financial support (Project: SR/S1/IC-51/2010). S.P. acknowledges the Council of Scientific and Industrial Research (CSIR), India for a fellowship. Crystal structure determination was performed at the DST-funded National Single Crystal Diffractometer Facility at the Department of Inorganic Chemistry, IACS.

REFERENCES

- (1) Gasco, A.; Schoenafinger, K. In *Nitric Oxide Donors*; Wang, P. G., Cai, T. B., Taniguchi, N., Eds.; Wiley-VCH: Weinheim, 2005; p 131–175.
- (2) Nirode, W. F.; Luis, J. M.; Wicker, J. F.; Wachter, N. M. *Bioorg. Med. Chem. Lett.* **2006**, *16*, 2299–2301.
- (3) Takayama, H.; Shirakawa, S.; Kitajima, M.; Aimi, N.; Yamaguchi, K.; Hanasaki, Y.; Ide, T.; Katsuura, K.; Fujiwara, M.; Ijichi, K.; Konno, K.; Sigeta, S.; Yokota, T.; Baba, M. *Bioorg. Med. Chem. Lett.* **1996**, *6*, 1993–1996.
- (4) Cerecetto, H.; Di Maio, R.; González, M.; Risso, M.; Saenz, P.; Seoane, G.; Denicola, A.; Peluffo, G.; Quijano, C.; Olea-Azar, C. *J. Med. Chem.* **1999**, *42*, 1941–1950.
- (5) Persichini, T.; Colasanti, M.; Fraziano, M.; Colizzi, V.; Medana, C.; Polticelli, F.; Venturini, G.; Ascenzi, P. *Biochem. Biophys. Res. Commun.* **1999**, *258*, 624–627.
- (6) Ghosh, P. B. *J. Chem. Soc. B* **1968**, 334–338.
- (7) Ghosh, P. B.; Whitehouse, M. W. *J. Med. Chem.* **1968**, *11*, 305–311.
- (8) Ghosh, P. B.; Whitehouse, M. W. *J. Med. Chem.* **1969**, *12*, 505–507.

- (9) Sheremetev, A. B.; Makhova, N. N.; Friedrichsen, W. In *Adv. Heterocycl. Chem.*; Katritzky, A. R., Ed.; Academic Press, 2001; Vol. 78, p 66–188.
- (10) Del Grosso, E.; Boschi, D.; Lazzarato, L.; Cena, C.; Di Stilo, A.; Fruttero, R.; Moro, S.; Gasco, A. *Chem. Biodivers.* **2005**, *2*, 886–900.
- (11) Takakis, I. M.; Tsantali, G. G.; Hass, G. W.; Giblin, D.; Gross, M. L. *J. Mass Spectrom.* **1999**, *34*, 1137–1153.
- (12) Wang, P. G.; Xian, M.; Tang, X.; Wu, X.; Wen, Z.; Cai, T.; Janczuk, A. J. *Chem. Rev.* **2002**, *102*, 1091–1134.
- (13) Bard, A. J., Ed. *Encyclopedia of Electrochemistry of the Elements*; Dekker: New York, 1974; Vol. Band 2.
- (14) Sreenath, K.; Thomas, T. G.; Gopidas, K. R. *Org. Lett.* **2011**, *13*, 1134–1137.
- (15) Sumalekshmy, S.; Gopidas, K. R. *Chem. Phys. Lett.* **2005**, *413*, 294–299.
- (16) Sreenath, K.; Suneesh, C. V.; Gopidas, K. R.; Flowers, R. A., II. *J. Phys. Chem. A* **2009**, *113*, 6477–6483.
- (17) Das, O.; Paria, S.; Paine, T. K. *Tetrahedron Lett.* **2008**, *49*, 5924–5927.
- (18) Peter de Lijser, H. J.; Fardoun, F. H.; Sawyer, J. R.; Quant, M. *Org. Lett.* **2002**, *4*, 2325–2328.
- (19) Everett, S. A.; Naylor, M. A.; Stratford, M. R. L.; Patel, K. B.; Ford, E.; Mortensen, A.; Ferguson, A. C.; Vojnovic, B.; Wardman, P. *J. Chem. Soc., Perkin Trans. 2* **2001**, 1989–1997.
- (20) Petrosyan, V. A.; Niyazymbetov, M. E.; Ul'yanova, É. V. *Russ. Chem. Bull.* **1990**, *39*, 546–550.
- (21) Thomas, J. R. *J. Am. Chem. Soc.* **1964**, *86*, 1446–1447.
- (22) Brokenshire, J. L.; Mendenhall, G. D.; Ingold, K. U. *J. Am. Chem. Soc.* **1971**, *93*, 5278–5279.
- (23) Brokenshire, J. L.; Roberts, J. R.; Ingold, K. U. *J. Am. Chem. Soc.* **1972**, *94*, 7040–7049.
- (24) Mendenhall, G. D.; Ingold, K. U. *J. Am. Chem. Soc.* **1973**, *95*, 2963–2971.
- (25) Niyazymbetov, M. E.; Ul'yanova, É. V.; Petrosyan, V. A. *Russ. Chem. Bull.* **1990**, *39*, 551–554.
- (26) Gowenlock, B. G.; Richter-Addo, G. B. *Chem. Soc. Rev.* **2005**, *34*, 797–809.
- (27) Mallory, F. B.; Cammarata, A. J. *Am. Chem. Soc.* **1966**, *88*, 61–64.
- (28) Bulacinski, A. B.; Scriven, E. F. V.; Suschitzky, H. *Tetrahedron Lett.* **1975**, 3577–3579.
- (29) Sebban, M.; Goumont, R.; Hallé, J. C.; Marrot, J.; Terrier, F. *Chem. Commun.* **1999**, 1009–1010.
- (30) Friedrichsen, W. *J. Phys. Chem.* **1994**, *98*, 12933–12937.
- (31) Stevens, J.; Schweizer, M.; Rauhut, G. *J. Am. Chem. Soc.* **2001**, *123*, 7326–7333.
- (32) Dunkin, I. R.; Lynch, M. A.; Boulton, A. J.; Henderson, N. *J. Chem. Soc., Chem. Commun.* **1991**, 1178–1179.
- (33) Hacker, N. P. *J. Org. Chem.* **1991**, *56*, 5216–5217.
- (34) Wolsey, W. C. *J. Chem. Educ.* **1973**, *50*, A335–A337.
- (35) Bodge, S.; MacDonnell, F. M. *Tetrahedron Lett.* **1997**, *38*, 8159–8160.
- (36) Ruiz, R.; Sanz, J.; Cervera, B.; Lloret, F.; Julve, M.; Bois, C.; Faus, J.; Muñoz, M. C. *J. Chem. Soc., Dalton Trans.* **1993**, 1623–1628.
- (37) Beaudoin, D. S.; Obare, S. O. *Tetrahedron Lett.* **2008**, *49*, 6054–6057.
- (38) Margiotta, N.; Bertolasi, V.; Capitelli, F.; Maresca, L.; Moliterni, A. G.; Vizza, F.; Natile, G. *Inorg. Chim. Acta* **2004**, *357*, 149–158.
- (39) Bruker, 2.1–0 ed.; Bruker AXS inc.: Madison, WI, 2006.
- (40) Otwinowski, Z.; Minor, W. In *Methods Enzymol.*; Carter, C. W., Jr. Sweet, R. M., Eds.; Academic Press: New York, 1997; Vol. 276, p 307–326.
- (41) Sheldrick, G. M. *SHELX-97, Programs for Crystal Structure Analysis (Release 97–2)*; University of Göttingen: Germany, 1998.
- (42) Watkin, D. M.; Pearce, L.; Prout, C. K. *CAMERON- A Molecular Graphics Package*, Chemical Crystallography Laboratory, University of Oxford: Oxford, 1993.
- (43) Farrugia, L. J. *J. Appl. Crystallogr.* **1999**, *32*, 837–838.
- (44) Addison, A. W.; Rao, T. N.; Reedijk, J.; van Rijn, J.; Verschoor, G. C. *J. Chem. Soc., Dalton Trans.* **1984**, 1349–1356.
- (45) Catalan, K. J.; Jackson, S.; Zubkowski, J. D.; Perry, D. L.; Valente, E. J.; Feliu, L. A.; Polanco, A. *Polyhedron* **1995**, *14*, 2165–2171.
- (46) Murphy, G.; Murphy, C.; Murphy, B.; Hathaway, B. *J. Chem. Soc., Dalton Trans.* **1997**, 2653–2660.
- (47) Murphy, G.; Nagle, P.; Murphy, B.; Hathaway, B. *J. Chem. Soc., Dalton Trans.* **1997**, 2645–2652.
- (48) Britton, D.; Mallory, F. B.; Mallory, C. W. *Acta Crystallogr.* **2002**, *CS8*, o235–o238.
- (49) Sakaguchi, U.; Addison, A. W. *J. Chem. Soc., Dalton Trans.* **1979**, 600–608.
- (50) Benedix, R.; Vogler, A. *Inorg. Chim. Acta* **1993**, *204*, 189–193.
- (51) Boyer, J. H.; Toggweiler, U. *J. Am. Chem. Soc.* **1957**, *79*, 895–897.
- (52) Luzyanin, K. V.; Gushchin, P. V.; Pombeiro, A. J. L.; Haukka, M.; Ovcharenko, V. I.; Kukushkin, V. Y. *Inorg. Chem.* **2008**, *47*, 6919–6930.
- (53) Brunner, H.; Loskot, S. *Angew. Chem., Int. Ed.* **1971**, *10*, 515–516.
- (54) Brunner, H.; Loskot, S. *J. Organomet. Chem.* **1973**, *61*, 401–414.
- (55) Becker, P. N.; Bergman, R. G. *J. Am. Chem. Soc.* **1983**, *105*, 2985–2995.
- (56) Becker, P. N.; Bergman, R. G. *Organometallics* **1983**, *2*, 787–796.
- (57) Chiu, W.-H.; Cheung, K.-K.; Che, C.-M. *J. Chem. Soc., Chem. Commun.* **1995**, 441–442.